

## Frequency modulated torsional resonance mode atomic force microscopy on polymers

Ayhan Yurtsever,<sup>1</sup> Alexander M. Gigler,<sup>1,a)</sup> Christian Dietz,<sup>2</sup> and Robert W. Stark<sup>1,b)</sup>

<sup>1</sup>Center for NanoScience (CeNS) and Department of Earth and Environmental Sciences,

Ludwig-Maximilians-Universität München, Theresienstraße 41, 80333 Munich, Germany

<sup>2</sup>Chemische Physik, Technische Universität Chemnitz, Reichenhainer Str. 70, 09107 Chemnitz, Germany

(Received 26 February 2008; accepted 19 March 2008; published online 8 April 2008)

In-plane mechanics of polymers can be probed by integrating frequency modulation and torsional resonance mode atomic force microscopy. We investigated a thin film of polystyrene-*block*-polybutadiene diblock copolymer. To gain more insight into image contrast formation, we examined displacement curves on polystyrene homopolymer surfaces of different molecular weights focusing on energy dissipation and frequency shift. Data suggest that the transition from a highly motile surface layer to the bulk material depends on the molecular weight of the polymer. This, in turn, indicates that the tip is slightly oscillating within the sample surface during imaging. © 2008 American Institute of Physics. [DOI: 10.1063/1.2907498]

The atomic force microscope (AFM) has become a standard instrument for imaging and characterization of polymers with nanometer resolution. Various AFM imaging techniques allow for mapping material properties to topographic surface features. Depending on the scheme of excitation, these techniques can be categorized as nonresonant methods, such as pulsed force mode,<sup>1,2</sup> or resonant methods such as phase imaging,<sup>3</sup> frequency modulation,<sup>4,5</sup> and time-resolved AFM.<sup>6,7</sup> All of these techniques are based on a flexural oscillation of the cantilever sensing forces perpendicular to the surface. The probe only interacts with the sample at the lower turning point of the cantilever oscillation and, thus, is far away from the surface for most of the oscillation cycle. In order to probe the in-plane mechanical properties of materials, the tip can also be driven to a small lateral instead of vertical oscillation. Such a lateral oscillation is used in imaging modes where the specimen is characterized by shear force interactions. Shear force imaging can be realized by applying a lateral modulation to a tip or sample with an amplitude of a few nanometers either while the tip is scanned across the specimen<sup>8</sup> or during approach/retract curves (displacement curves).<sup>9,10</sup> Using higher excitation frequencies close to the torsional resonances (TR) of the cantilever,<sup>11</sup> in-plane conservative (elasticity under shear) as well as dissipative (friction) properties can be determined. Even without the need for active driving of the TR, in-plane elastic properties can be extracted from the thermomechanical oscillations of the force sensor in contact with the surface.<sup>12</sup>

In order to achieve a well-defined lateral tip oscillation, the TR mode has been introduced where two piezoelectric elements force the cantilever to a torsional oscillation.<sup>13</sup> To provide high sensitivity together with stable imaging, frequency modulation techniques can be applied to TR mode.<sup>14,15</sup> However, the fundamental mechanisms of image formation in this mode demand further investigation. We therefore discuss frequency modulated TR mode

AFM (FM-TR-AFM) for imaging thin polymer films in the following.

The experiment was set up using a Dimension 3100 AFM with a NanoScope IV controller equipped for TR-mode operation (Veeco Metrology Inc., Santa Barbara, CA). The control loop was extended by a phase-locked loop electronics (Easy-PLL, Nanosurf AG, Liestal, Switzerland), as shown in Fig. 1. Silicon cantilevers (ZEIHR, Nanosensors, Neuchâtel, Switzerland) with torsional resonant frequencies below 1 MHz were used (flexural resonance of 117 kHz, TR of 910 kHz, and flexural spring constant 27 N/m). A positive feedback of the lateral signal of the photodiode together with an automatic gain control was implemented for driving the cantilever into a stable torsional oscillation. The detuning ( $\Delta f$ ) of the TR was utilized for topographic feedback. Two different modes of operation were used: constant amplitude (CA) mode for imaging and constant excitation (CE) mode for displacement curves. In CA mode, the energy needed to maintain the torsional oscillation amplitude constant pro-

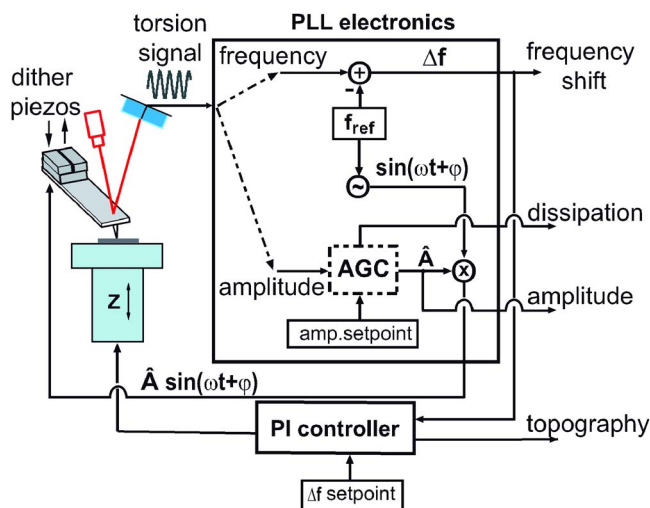


FIG. 1. (Color online) Scheme of frequency modulated torsional resonance mode AFM. A positive feedback of the photodiode signal is used to drive the dither piezos for torsional excitation. Frequency shift, energy dissipation, and oscillation amplitude can be concurrently measured with the topography.

<sup>a)</sup>Author to whom correspondence should be addressed. Electronic mail: gigler@lmu.de. Tel.: +49 89 2180 4185. FAX: +49 89 2180 4334.

<sup>b)</sup>Electronic mail: stark@lmu.de.

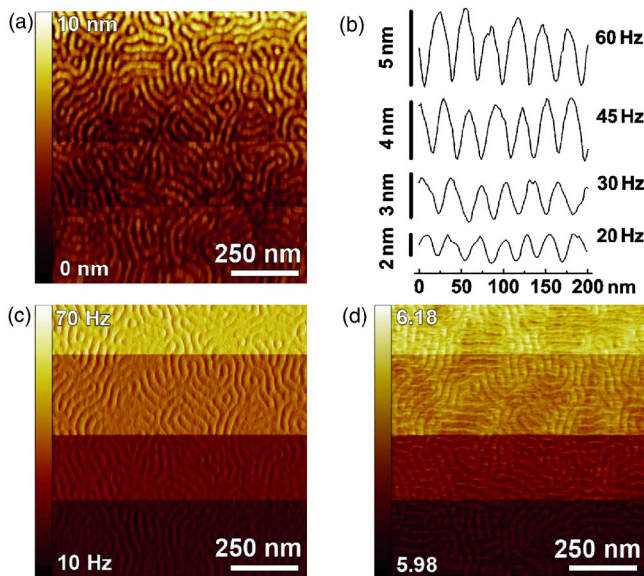


FIG. 2. (Color online) Dependence of image contrast on the detuning set point in CA mode. The detuning set point was varied in steps (20, 30, 45, and 60 Hz from bottom to top). Representative cross sections from each region are shown in (b). (c) Frequency shift (error) image and (d) energy dissipation image.

vides a direct measure for energy dissipation at the tip-sample contact.

To demonstrate the capabilities of the frequency modulation technique in TR mode AFM, we imaged a thin film of polystyrene-*block*-polybutadiene (SB) diblock copolymer (Polymer Source Inc., Dorval Montreal, Canada) with molecular weights  $M_{w,PS}=13.6$  kg/mol and  $M_{w,PB}=33.7$  kg/mol (PS is polystyrene and PB is polybutadiene). For sample preparation, the polymer was dissolved in toluene (concentration 30 mg/ml) and spin coated onto pieces of a silicon wafer. Prior to coating, the substrates were cleaned by sonication with acetone, ethanol, and toluene for 15 min each and dried in a stream of nitrogen afterwards. Spin coating at 1000 rpm resulted in a 150-nm-thick film of SB with a structure of cylinders of PS lying parallel to the surface. The thickness was determined by measuring the height profile of a scratch.

For imaging of SB, the CA scheme of the FM-TR mode was used. The cantilever was oscillated with small amplitude (below 2 nm) parallel to the sample surface. In order to elucidate the effect of the detuning set point on image contrast, the set point was varied stepwise from 20 to 60 Hz. Figure 2(a) shows the topography together with representative cross sections [Fig. 2(b)] for each region of interest. Since the PB block is more compliant compared to the PS block, PS appeared higher (brighter color) in the topography image. The topographic image showed the typical structure of cylinders oriented parallel to the substrate.<sup>16</sup> The height difference between PS and PB increased from 2 nm (20 Hz set point), 3 nm (30 Hz), 4 nm (45 Hz), to 5 nm (60 Hz), since the material was increasingly compressed due to the effective average force exerted by the tip. As the frequency shift was used as a control parameter for the  $z$ -feedback loop, Fig. 2(c) reflects the feedback response only. Energy dissipation [Fig. 2(d)], however, allows discerning of the polymer blocks. It correlates with the amount energy needed to maintain the oscillation amplitude constant (CA mode). With the increase in frequency shift set point, we observed a shift to

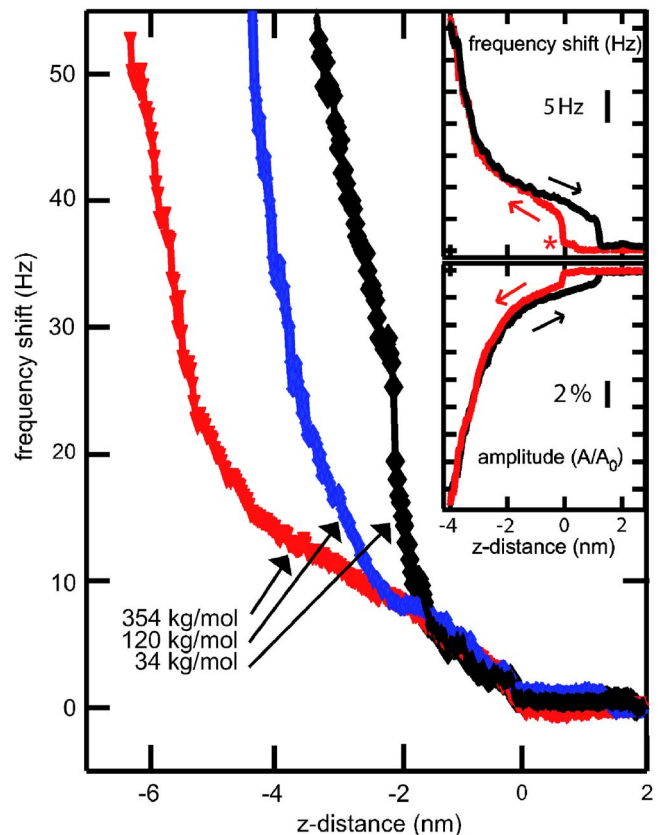


FIG. 3. (Color online) Detuning vs distance plots of the torsional oscillation acquired in CE mode on PS homopolymers with  $M_w=34.3$  kg/mol (black), 119.6 kg/mol (blue), and 354.0 kg/mol (red). The inset shows a typical displacement curve on PS (119.6 kg/mol) with frequency shift and amplitude of the torsional oscillation as a function of  $z$ -actuator displacement, respectively. Approach (red) and retract (black) are also indicated by the arrows. The asterisk marks the jump of the AFM tip to contact with the sample.

higher values of dissipation, i.e., the PB domains appeared brighter in this image since more deformation energy was turned into heat.

Lacking a rigid theoretical description of the indentation process of a torsionally vibrating tip into a polymeric material, we attempted to understand the image formation from an experimental point of view. Hence, displacement curves of the torsional resonance detuning versus  $z$  position as well as torsional oscillation amplitude versus  $z$  position were conducted on PS homopolymer surfaces (Polymer Source Inc., Dorval Montreal, Canada) with different molecular weights ( $M_w=34.3$ , 119.6, and 354.0 kg/mol). Similar to the SB samples, the polymer samples were prepared by spin coating from a toluene solution with a concentration of 20 mg/ml onto freshly cleaned pieces of a silicon wafer, which resulted in a film thickness of 150 nm for all samples. Cleaning equaled the procedure described above.

Displacement curves (frequency shift and amplitude change versus  $z$  position recorded in CE mode), as shown in the inset of Fig. 3, revealed details of the interaction between the tip and the sample. At close proximity, the tip snapped into contact with the surface (asterisk). The snap in was accompanied by a sharp change in amplitude and detuning. Over the next 2 nm, amplitude and frequency slowly varied. At a displacement of more than 3 nm, both amplitude and frequency rapidly changed. Upon retraction, a hysteresis of frequency shift and amplitude prevailed. We observed a posi-

tive frequency shift and decreased amplitude due to contact stiffening. The initial slope of the frequency shift plot was rather linear. This can be explained by mobile polymer coils close to the polymer/air interface. Indenting further, the tip penetrated through the first layer exerting shear stress on the bulk polymer. With the increasing indentation, more and more material was involved in tip-sample interaction. This led to an increased frequency shift which may be attributed to polymer entanglements,<sup>17,18</sup> limiting the chain mobility in the bulk.

In order to assess this effect of the polymer chain length, displacement curves focusing on frequency shift were measured on different PS homopolymers ( $M_w=34.3$ , 119.6, and 354.0 kg/mol), as shown in Fig. 3. For all specimens, two regimes were observed in the displacement curves: Firstly, a rather compliant surface layer was probed; secondly, the less mobile bulk of the polymer was sensed by the oscillatory motion of the tip. The position of the kink between the two regimes strongly correlated with the molecular weight of the homopolymer.

The approach-retract response of amplitude reduction and frequency shift of the torsional oscillation can be related to the mechanical properties of the thin film. As we observed two distinct regions of different mechanical behavior in terms of periodic shear stress, a mobile thin layer followed by a more rigid bulk seems a reasonable assumption. The apparent stratification of the film may be caused by the segregation of short and long chained molecules at the interfaces of a film, since short chains (low  $M_w$ ) are repelled from the bulk (higher  $M_w$ ) due to entropic forces. Even purified homopolymers yet having a finite polydispersity of 1.05, such as the polymers used in our experiments, result in a superficial layer consisting of the shorter molecules.

In summary, FM-TR-AFM is a powerful tool for imaging polymeric samples with spatially varying mechanical properties. The indentation experiments clearly show that the tip is oscillating within the motile top layer of the polymer surface even for detuning on the order of 10 Hz. For the diblock copolymer, this means that while imaging in FM-TR-AFM, the tip is also compressing the different polymer blocks according to their compliance. This effect causes an apparent increase of topography with the detuning set point. Furthermore, we investigated frequency shift versus distance curves on PS, which revealed two different interaction regimes. Depending on the molecular weight, we

observed a distinct change in the signature of the distance curves. Hence, we propose a stratified structure due to the segregation of shorter chains from longer chains and, thus, a resulting two layer behavior. Our findings show that FM-TR-mode spectroscopy enables discerning of polymer samples by their different molecular weight.

We gratefully acknowledge financial support by the German Federal Ministry of Education and Research (BMBF) Grant Nanofutur 03N8706 and by the European Commission (FORCETOOL, NMP4-CT-2004-013684). The authors thank Robert Magerle for fruitful discussions. A.Y. was supported by the Doctorate Program Nano-Bio-Technology (IDK-NBT) of the Elite Network of Bavaria, International and A.M.G. was financed by the cluster of excellence "Nanosystems Initiative Munich (NIM).

<sup>1</sup>H. U. Krottil, T. Stifter, and O. Marti, *Rev. Sci. Instrum.* **71**, 2765 (2000).

<sup>2</sup>A. Gigler, C. Gnahn, O. Marti, T. Schimmel, and S. Walheim, *J. Phys.: Conf. Ser.* **61**, 346 (2007).

<sup>3</sup>S. N. Magonov, V. Elings, and M. H. Whangbo, *Surf. Sci.* **375**, L385 (1997).

<sup>4</sup>F. Dubourg, G. Couturier, J. P. Aime, S. Marsaudon, P. Leclere, R. Lazzaroni, J. Salardenne, and R. Boisgard, *Modell. Simul. Mater. Sci. Eng.* **167**, 177 (2001).

<sup>5</sup>F. Dubourg, S. Kopp-Marsaudon, P. Leclere, R. Lazzaroni, and J. P. Aime, *Eur. Phys. J. E* **6**, 387 (2001).

<sup>6</sup>M. Stark, R. W. Stark, W. M. Heckl, and R. Guckenberger, *Proc. Natl. Acad. Sci. U.S.A.* **99**, 8473 (2002).

<sup>7</sup>O. Sahin, S. Magonov, C. Su, C. F. Quate, and O. Solgaard, *Nat. Nanotechnol.* **2**, 507 (2007).

<sup>8</sup>H. U. Krottil, E. Weilandt, T. Stifter, O. Marti, and S. Hild, *Surf. Interface Anal.* **27**, 341 (1999).

<sup>9</sup>H. U. Krottil, T. Stifter, and O. Marti, *Appl. Phys. Lett.* **77**, 3857 (2000).

<sup>10</sup>H. U. Krottil, T. Stifter, and O. Marti, *Rev. Sci. Instrum.* **72**, 150 (2001).

<sup>11</sup>M. Reinstädler, U. Rabe, V. Scherer, U. Hartmann, A. Goldade, B. Bhushan, and W. Arnold, *Appl. Phys. Lett.* **82**, 2604 (2003).

<sup>12</sup>T. Drobek, R. W. Stark, and W. M. Heckl, *Phys. Rev. B* **64**, 045401 (2001).

<sup>13</sup>L. Huang and C. M. Su, *Ultramicroscopy* **100**, 277 (2004).

<sup>14</sup>A. Yurtsever, A. M. Gigler, E. Macias, and R. W. Stark, *Appl. Phys. Lett.* **91**, 253120 (2007).

<sup>15</sup>A. Yurtsever, A. M. Gigler, and R. W. Stark, *J. Phys.: Conf. Ser.* **100**, 052033 (2008).

<sup>16</sup>A. Knoll, A. Horvat, K. S. Lyakhova, G. Krausch, G. J. A. Sevink, A. V. Zvelindovsky, and R. Magerle, *Phys. Rev. Lett.* **89**, 035501 (2002).

<sup>17</sup>F. Dubourg, J. P. Aime, S. Marsaudon, G. Couturier, and R. Boisgard, *J. Phys.: Condens. Matter* **15**, 6167 (2003).

<sup>18</sup>H. R. Brown and T. P. Russell, *Macromolecules* **29**, 798 (1996).